

Ca II Triplet Spectroscopy of Giants in SMC Star Clusters: Abundances, Velocities and the Age-Metallicity Relation

G. S. Da Costa

Mount Stromlo and Siding Spring Observatories, The Australian National University, Private Bag, Weston Creek Post Office, ACT 2611, Australia

Electronic mail: gdc@mso.anu.edu.au

and

D. Hatzidimitriou

Physics Department, University of Crete, P.O. Box 2208, Heraklion 710 03, Crete, Greece

Electronic mail: dh@physics.ucl.gr

ABSTRACT

We have obtained spectra at the Ca II triplet of individual red giants in seven SMC star clusters whose ages range from ~ 4 to 12 Gyr. The spectra have been used to determine mean abundances for six of the star clusters to a typical precision of 0.12 dex. When combined with existing data for other objects, the resulting SMC age-metallicity relation is generally consistent with that for a simple model of chemical evolution, scaled to the present-day SMC mean abundance and gas mass fraction. Two of the clusters (Lindsay 113 and NGC 339), however, have abundances that are ~ 0.5 dex lower than that expected from the mean age-metallicity relation. It is suggested that the formation of these clusters, which have ages of ~ 5 Gyr, may have involved the infall of unenriched gas, perhaps from the Magellanic Stream. The spectra also yield radial velocities for the seven clusters. The resulting velocity dispersion is 16 ± 4 km s $^{-1}$, consistent with those of the SMC planetary nebula and carbon star populations.

Subject headings: galaxies: abundances — galaxies: individual (SMC) — galaxies: kinematics and dynamics — galaxies: star clusters — Magellanic Clouds

Accepted for Publication in *The Astronomical Journal*

1. Introduction

The age-metallicity relation of a stellar system is one of the fundamental diagnostics through which we can learn about the chemical enrichment processes that occur during the system’s evolution. Within the solar neighbourhood for example, it is possible to determine the age-metallicity relation for the Galactic disk from the ages and metallicities of field stars (e.g., Edvardsson *et al.* 1993), and modelling of this relation and its scatter suggests a complex evolution involving gas inflow and the radial diffusion of orbits in the presence of a radial abundance gradient (e.g., Pagel & Tautvaisiene 1995). However, for more distant systems, we can no longer use individual F- and G-type dwarfs to determine ages and abundances. Instead we must use star clusters since, at least in principle, it is relatively straightforward to determine a cluster’s age and abundance. In particular, for our nearest galactic neighbors it is possible to constrain cluster ages via main sequence turnoff luminosities even if the clusters are as old as the galactic halo globular clusters. Thus provided clusters of all ages can be found, which is of course a function of formation and destruction processes, the age-metallicity relations of these nearby systems can be fully outlined.

It is with this proviso, however, that a major difficulty often arises. For example, in the Large Magellanic Cloud (LMC) there is a well established population of old metal-poor star clusters whose properties are comparable to the galactic halo globular clusters (e.g., Suntzeff *et al.* 1992). There is also a large population of intermediate-age clusters, but the ages of these clusters are all less than 3 – 4 Gyr (e.g., Da Costa 1991, Olszewski *et al.* 1996, Geisler *et al.* 1997) and only a single cluster, ESO 121-SC03 (Mateo *et al.* 1986) is known to fall in the “age gap” between the old and intermediate-age objects. As emphasized by Olszewski *et al.* (1996), for example, this gap in the LMC cluster age distribution also represents an “abundance gap”, in that the old clusters are all metal-poor while the intermediate-age clusters are all relatively metal-rich (Olszewski *et al.* 1991), approaching even the present-day abundance in the LMC. Yet because of the lack of clusters older than ~ 3 Gyr, we have essentially no constraints on the timescale for what was the major enrichment event in the LMC’s history. The Small Magellanic Cloud (SMC), on the other hand, is known to have a different distribution of cluster ages from the LMC (e.g., Da Costa 1991). In particular, while the number of clusters with ages determined from main sequence turnoff photometry is smaller than for the LMC, there is no sign in these data for any substantial “age gap”. Thus, in principle, the SMC age-metallicity relation defined by the star clusters can cover from the present day back almost to the age of the oldest galactic halo globular clusters¹.

The SMC age-metallicity relation, as it stood prior to the present work (e.g., Stryker *et al.* 1985, Da Costa 1991, Olszewski *et al.* 1996) had fundamentally two components. First, it appeared that following a presumed initial burst of star formation that brought the cluster abundances up to $[\text{Fe}/\text{H}] \approx -1.3$, the subsequent net rate of enrichment was very low until perhaps 2 – 3 Gyr

¹NGC 121, the oldest SMC star cluster for which age information exists, is perhaps 2 – 3 Gyr younger than the galactic halo globular clusters (e.g., Stryker *et al.* 1985).

ago. Second, commencing at an age of $\sim 2 - 3$ Gyr, the rate of enrichment apparently increased to bring the cluster abundances up to the present-day SMC abundance of $[\text{Fe}/\text{H}] \approx -0.6$ dex. This sort of age-metallicity relation is very different from that of the solar neighbourhood and it also differs substantially from that expected from the simple model of chemical evolution. As summarized by Dopita (1991), the first component of this relation could be explained if the infall rate of unenriched gas matched the rate of chemical enrichment, or if the newly synthesized metals were lost in a strong galactic wind (or a combination of these processes). The second component could result from the cessation of these processes, or from an increased star formation rate perhaps as a result of an interaction with the LMC. However, it must be emphasized that the majority of the cluster abundances used to define this age-metallicity relation are rather uncertain: most are derived from the color of the cluster red giant branch in the color-magnitude diagram. This technique depends on the reddening of the cluster and on the zeropoint of the photometry, and it also contains the uncertainty inherent in the calibration of a parameter that is sensitive to both age and abundance.

It is obvious then that to verify the chemical history of the SMC implied by this age-metallicity relation, it needs to be redetermined using a consistent, accurate and reddening independent method. Spectroscopy at the Ca II triplet of globular cluster red giants analyzed in terms of the magnitude difference from the horizontal branch is such a method (see, for example, Da Costa & Armandroff 1995, Rutledge *et al.* 1997 and the references therein), and as Olszewski *et al.* (1991) have shown, it can be extended to red giants in intermediate-age star clusters since the higher gravity of the younger stars has little effect, at least for ages in excess of perhaps 2 Gyr. The purpose of this paper then is to present Ca II triplet spectroscopy for red giants in a number of SMC star clusters and to discuss the implications of these new results for the SMC age-metallicity relation and the SMC chemical history. Spectroscopy of individual stars has the added bonus that we can also determine the cluster radial velocities. The kinematics of the LMC cluster system has produced some intriguing results (e.g., Schommer *et al.* 1992) and while the sample of clusters observed here is small, the velocity results can nevertheless be compared with the kinematics of other SMC populations.

The outline of the remainder of the paper is as follows: in the following section the sample of SMC clusters observed, the data reduction procedure, and the line strength and radial velocity analysis techniques are described. Section 3 discusses in some detail the derivation of abundances from the observed line strengths. Then, in the first part of Sect. 4, the kinematics implied by the cluster radial velocities are derived and compared with those of other SMC populations with similar ages. In the second part of this section (Sect. 4.2) the full SMC age-metallicity relation is constructed. The implications of this relation for the chemical evolution of the SMC are discussed in the final section.

2. Observations and Reductions

2.1. The SMC Cluster Sample

Compared to the LMC, there are fewer well-studied star clusters in the SMC, though as noted above, the SMC clusters do not show the large “age-gap” exhibited by the LMC cluster population. For this reason we initially selected only those clusters with both good quality color-magnitude (c-m) diagrams and ages, as determined from main sequence turnoff photometry, greater than ~ 2 Gyr. There are six such clusters: Lindsay 1 (Olszewski *et al.* 1987), Kron 3 (Rich *et al.* 1984), Lindsay 11 (Mould *et al.* 1992), NGC 121 (Stryker *et al.* 1985), NGC 339 (Olszewski, 1994, priv. comm.), and Lindsay 113 (Mould *et al.* 1984). For each cluster the brighter half dozen or so candidate cluster red giants were selected for spectroscopic observation at the Ca II triplet. In this selection process we were careful to ensure that none of the stars chosen had been previously identified via IR-photometry and/or low resolution spectroscopy as upper-AGB stars (whether of C, M or S spectral type). Then, in order to increase the sample, we constructed a second list of SMC clusters for which main sequence turnoff color-magnitude diagrams were not available, but for which independent data suggested an age in the $\gtrsim 2$ Gyr to 12 Gyr range. The only cluster in this second list for which stars were actually observed was NGC 361. Arp (1958) gives a photographic c-m diagram for this cluster but it does not reach as faint as even the expected magnitude for the core helium burning stars. It therefore yields little age information. However, when corrected for the effects of a superposed bright star (cf. van den Bergh 1981) the integrated *UBV* colors of NGC 361 are similar to those of the six clusters in the first list. Thus it is likely that NGC 361 is of intermediate-age, and the brighter red giants from the c-m diagram of Arp (1958) were added to the sample for spectroscopic study.

2.2. Observations

The program stars were observed with the Anglo-Australian Telescope using the RGO spectrograph with the 25cm camera and a Tek 1k CCD, during runs in 1992 September (second halves of five nights) and 1994 August (second halves of two nights). The instrumental setup was identical to that discussed in Da Costa & Armandroff (1995, hereafter DA95) which can be consulted for a more detailed description. In brief, the spectra cover the wavelength interval $\sim 7700\text{--}9300\text{\AA}$ at a resolution of $\sim 3\text{\AA}$. Total exposure times for the SMC cluster stars ranged from 800 seconds to 2 hours for the faintest stars. Wherever possible two stars were observed simultaneously by rotating the spectrograph slit to an appropriate position angle. Standard IRAF² procedures were used to generate sky-subtracted wavelength-calibrated spectra from the raw data. Some examples of the final spectra are shown in Fig. 1. Spectra of galactic globular cluster red giants obtained during these observing runs are discussed in DA95, who have demonstrated

²IRAF is distributed by the National Optical Astronomy Observatories, which is operated by the Association of Universities for Research in Astronomy, Inc. (AURA) under cooperative agreement with the National Science Foundation.

that the data from the two observing runs have no systematic differences and can be used interchangeably. At this point it is also worth mentioning that Lindsay 11 star 1 from Mould & Aaronson (1982) was also observed during the 1994 August run. This star has the infra-red colors of an upper-AGB carbon star (cf. Mould & Aaronson 1982) and the presence of strong CN-bands at $\lambda \approx 7850\text{\AA}$ and 8050\AA in the spectrum confirm this classification. Such bands were not seen in the spectrum of any other star observed. There were also no indications in these spectra of TiO bands whose presence can affect the measurement of the Ca II triplet line strength (e.g., Olszewski *et al.* 1991).

2.3. Line Strength Measurements

The (pseudo) equivalent widths of the two stronger lines of the Ca II triplet, $\lambda 8542\text{\AA}$ and $\lambda 8662\text{\AA}$, were measured from the red giant spectra by applying the gaussian fitting technique of DA95 (see also Armandroff & Da Costa 1991). The sum of these line strength measures, denoted by $W_{8542}+W_{8662}$, was then computed for each observation. Final values for 33 stars in the fields of the 7 SMC clusters are given in Table 1. In this table the errors accompanying the $W_{8542}+W_{8662}$ values are those which result from the uncertainties in the parameters that define the gaussian line profile fits. Comparison of these errors with the mean single observation error in $W_{8542}+W_{8662}$ derived from the 31 repeat observations of 15 stars shows that these gaussian line profile fit uncertainties probably overestimate the true errors by perhaps 25 percent (0.32\AA versus 0.40\AA). Nevertheless, we have been conservative and retained the individual gaussian line profile fit uncertainties.

For four of the seven clusters, the available photometry is in the B and R bandpasses, whereas the abundance calibration procedure (cf. DA95) requires V magnitudes for both the individual stars and for the horizontal branch luminosity. To overcome this situation we have made use of the empirical transformation:

$$B - V = (0.685 \pm 0.005)(B - R) - (0.06 \pm 0.01) \quad (1)$$

This transformation is based on high quality photoelectric BVR photometry of red giants in the galactic globular clusters 47 Tuc, NGC 288, NGC 362, NGC 6397 and NGC 6752 (E. M. Green, 1987, priv. comm.) and is appropriate for the reddening $E(B-V) = 0.04$ mag assumed for the SMC clusters. The rms deviation about the fitted line is only 0.010 mag and the equation is valid between $B - R \approx 1.1$ ($B - V \approx 0.7$) and $B - R \approx 2.5$ ($B - V \approx 1.65$). The V magnitude for each program star then follows from the observed B magnitude and the computed $B - V$ color. The same process has also been used to fix the V_{HB} values for these clusters: the median $B - R$ color of the red clump of core helium burning stars (which constitutes the horizontal branch in these clusters) was converted to $B - V$ via equation (1) and combined with B_{HB} , taken as R_{HB} plus the median $B - R$ color, to generate V_{HB} . This process can be verified for two of the four clusters involved since independent BV photometry is available. For Kron 3, the c-m diagram

of Gascoigne (1980) suggests $V_{HB} \approx 19.3$ while Alcaïno *et al.* (1996) list $V_{HB} = 19.50 \pm 0.05$. Both these values are in agreement with our adopted value of 19.44 derived from the $(R, B - R)$ photometry of Rich *et al.* (1984). We note also that the Lindsay 1 c-m diagram in Gascoigne (1980) gives $V_{HB} \approx 19.3$, again in good accord with our value $V_{HB} = 19.20$ adopted from the $(V, B - V)$ photometry of Olszewski *et al.* (1987). For NGC 121, the photometry of Tifft (1963) for zones 2 and 3, which should be free of photographic background effects (cf. Stryker *et al.* 1985), gives $V_{HB} \approx 19.6$. This agrees well with the value $V_{HB} = 19.60$ derived from the $(R, B - R)$ photometry of Stryker *et al.* (1985). The adopted V_{HB} values for all the sample clusters (except NGC 361 for which no suitable photometry exists) are given in Table 2.

In Fig. 2 the line strength measures are plotted against the V magnitude difference from the horizontal branch, $V - V_{HB}$, for all stars observed in the fields of 6 of the 7 clusters in the sample. The lack of a c-m diagram reaching faint enough to reveal the magnitude of the horizontal branch (or red clump) in NGC 361 precludes analysis of the line strengths for this cluster. The galactic globular cluster calibration lines in this Figure have been taken from DA95 and the panels of this diagram provide one indication of the cluster membership status for each of the stars observed. Since there is no reason to suspect that any of these clusters contain a substantial internal abundance range, we can assume that any star whose Ca II triplet line strength lies significantly away from those of the majority, is not likely to be a member of that cluster. Inspection of Fig. 2 shows that the star MJD240 in the field of Lindsay 11 has such a discrepant line strength, while all other stars appear, on this basis at least, to be members of their respective clusters. An additional, and independent, means to investigate cluster membership status is provided by the comparatively large heliocentric velocity of the SMC. The measurement of radial velocities from the observed spectra will be discussed in Sect. 2.4, but for the moment we note that all stars except Lindsay 11 MJD240 and NGC 121 SDM029 have radial velocities consistent with not only SMC membership but also membership in their respective clusters. Lindsay 11 MJD240 is apparently an SMC field star while the low radial velocity of NGC 121 SDM029 indicates that this star is probably a foreground Galactic star. This star, and Lindsay 11 MJD240, will not be considered further.

As shown by a number of authors (e.g., DA95, Rutledge *et al.* 1997, and the references therein), the slope of the relation between the Ca II line strength index $W_{8542} + W_{8862}$ and $V - V_{HB}$ is independent of abundance, at least for $V - V_{HB} \lesssim -0.5$ mag. Thus the individual line strength measures for the stars observed in a cluster can be combined into a single quantity, the reduced equivalent width, denoted by W' . W' can then be calibrated in terms of metal abundance. On the system of DA95 which we follow here, W' is defined as the mean value of the quantity $W_{8542} + W_{8862} + 0.62(V - V_{HB})$ for the stars observed in a particular cluster. Since we have now established the cluster membership status of the program stars, we can compute W' for each cluster. The resulting values are listed in Table 2. We note that for the clusters Lindsay 1, Kron 3 and NGC 339, the cluster W' value is simply the mean of the stellar values since the individual $W_{8542} + W_{8862}$ errors are all similar. For the other three clusters, however, this is not the case and

the value of W' was computed as a weighted average, with the weights taken as the inverse square of the $W_{8542}+W_{8862}$ errors given by the gaussian line profile fit uncertainties for each individual star. We note also that the error listed with the W' values in Table 2 contains not only the error, as expressed by the standard error in the mean, from the scatter of the individual values, but also includes the effect of an assumed ± 0.10 mag uncertainty in the value of V_{HB} for each cluster.

For the three clusters where the value of W' was computed as a weighted average, it is of interest to see if the values change significantly if different weighting schemes are adopted. Consequently, we have computed values of W' for these clusters for the case of no weighting, and for a weighting scheme in which the observed mean single observation error in $W_{8542}+W_{8862}$ (0.32 Å) together with the number of observations per star was used to compute the weights. We find that in each of these cases, the values of W' computed for the three clusters agree with those given in Table 2 to well within the uncertainties listed in the Table. The uncertainties in the alternate W' values are also comparable to those given in Table 2 except for the case of Lindsay 113 and no weighting. Here the outliers (cf. Fig. 2), whose larger errors are ignored in this particular calculation, generate an uncertainty that is a factor of two larger than that listed in Table 2. We believe, however, that the values listed in Table 2 are the appropriate ones to adopt. The relation between these W' values and abundance will be discussed in Section 3.

2.4. Radial Velocities

The determination of radial velocities from the spectra obtained in these observing runs has been discussed in detail in DA95. Briefly, the program star spectra were cross-correlated with high S/N spectra of bright G- and K-type giant radial velocity standards. The velocity zeropoint for each run was set by minimizing, after applying heliocentric corrections, the difference between the observed and standard velocities for both the radial velocity standards and a number of galactic globular cluster stars with well determined velocities (see DA95 for details). The resulting uncertainty in the zeropoint of the velocity system is ~ 2 km s⁻¹. Based on the repeat observations, the individual radial velocity determinations for our program stars have an average error of 6 km s⁻¹.

In Table 2 we give mean heliocentric velocities for the 7 SMC star clusters observed. These means were calculated from the individual cluster star observations and the tabulated errors are the standard deviations of the mean for the samples. An external check on these velocities is provided by the cluster NGC 121 for which other radial velocity determinations exist. Zinn & West (1984) find 139 ± 20 km s⁻¹ (after a zeropoint shift of -5 km s⁻¹, see Hesser *et al.* 1986) while Hesser *et al.* (1986) list $V_r = 138 \pm 15$ km s⁻¹. Both determinations are based on integrated spectra of the cluster. Suntzeff *et al.* (1986) give $V_r = 126 \pm 15$ km s⁻¹ for a single red giant believed to be a member of NGC 121, while more recently, Dubath *et al.* (1997) have determined $V_r = 147 \pm 2$ km s⁻¹ for NGC 121, again from an integrated cluster spectrum. All these values are in good accord with our determination for this cluster of $V_r = 138 \pm 4$ km s⁻¹, based on the

velocities of four cluster red giants. The kinematics of this sample of old and intermediate-age clusters will be discussed in Sect. 4.1.

3. Cluster Abundances

In their paper DA95 give a calibration of W' with abundance using $[\text{Fe}/\text{H}]$ values for galactic globular clusters that have their origin with Zinn & West (1984). There is an excellent correlation between W' and $[\text{Fe}/\text{H}]_{\text{ZW84}}$ though it is not linear over the entire $[\text{Fe}/\text{H}]_{\text{ZW84}}$ range exhibited by the clusters. DA95 chose to model the relation by two linear segments that join at $W' = 3.8\text{\AA}$ or $[\text{Fe}/\text{H}]_{\text{ZW84}} = -1.44$, finding a rms dispersion about the fitted lines of ≤ 0.09 dex. There are, however, a number of issues that must be addressed before we can convert the SMC cluster W' values in Table 2 to abundance, using a calibration such as that of DA95.

The first of these is relatively straightforward. The definition of W' uses the difference between the apparent magnitude of the red giant and that of the horizontal branch. In the DA95 analysis, for example, the V_{HB} values used are those of globular cluster core helium burning stars, i.e., stars whose age is ~ 15 Gyr. The majority of the clusters studied here, however, have ages considerably younger than the galactic globular clusters. Now, as shown by, for example, the isochrones of Bertelli *et al.* (1994), at fixed abundance the luminosity of core helium burning stars becomes progressively brighter as age decreases or, more physically, as turnoff mass increases. For example, at an abundance of $Z=0.001$ ($\log Z/Z_{\odot} = -1.3$), the initial M_V of core helium burning stars at an age of 4 Gyr is 0.28 mag brighter than it is at 15 Gyr (Bertelli *et al.* 1994). Thus the observed $V - V_{\text{HB}}$ value for a red giant in a younger cluster is smaller than it would be in a cluster as old as the galactic globulars. Failure to allow for this effect would give rise to an overestimate of the true cluster abundance with the difference systematically increasing with decreasing cluster age. Consequently, for a given abundance calibration (see below), we will tabulate two abundances for each cluster, one based on the observed value of W' and a second derived from a corrected value of W' . The correction to W' comes from using the adopted cluster ages given in Table 2 with Bertelli *et al.* (1994) isochrones of appropriate abundance to estimate the change in V_{HB} . An independent calculation of this effect using the models of Seidel *et al.* (1987b) in conjunction with the Revised Yale Isochrones (Green *et al.* 1987), as described in Hatzidimitriou (1991), gives essentially identical results.

The second issue involves the fact that W' is a *calcium* line strength index whereas the calibration is to $[\text{Fe}/\text{H}]$ values. As long as there is no difference in $[\text{Ca}/\text{Fe}]$ between the program and calibration objects, this is not a matter for concern. However, calcium, being an α -element, has its origin primarily in SNeII and is enhanced, relative to the solar ratio, in both globular cluster and metal-poor galactic halo stars (e.g., Wheeler *et al.* 1989). Iron enrichment, on the other hand, is thought to occur primarily from SNeIa which have a longer evolutionary time than SNeII. Thus the $[\text{Ca}/\text{Fe}]$ ratio is quite likely to be a function of star formation and enrichment history. In particular, a star in an SMC cluster with an age half that, or less, of the galactic

globular clusters is not likely to have the same $[\text{Ca}/\text{Fe}]$ value as a galactic globular cluster star, even though they may have the same $[\text{Fe}/\text{H}]$. At the present time we can do little about this issue other than to note first, that investigation of element abundance ratios in SMC and LMC intermediate-age and old cluster and field stars is likely to be a prime science project for the coming 8m class telescopes in the southern hemisphere, and second, that in young SMC field stars the $[\alpha/\text{Fe}]$ ratio is approximately solar despite the moderate overall Fe depletion (e.g., Hill 1997, Luck & Lambert 1992). As regards our own data, two points can be made: first, interpreting W' with a galactic globular cluster based relation (i.e., one for which $[\text{Ca}/\text{Fe}] \approx +0.3$) will lead to an *underestimate* of the true $[\text{Fe}/\text{H}]$ if $[\text{Ca}/\text{Fe}] \leq 0.3$ in the program stars. In such a case the derived $[\text{Fe}/\text{H}]$ values will represent lower limits on the actual abundance value. Second, it would seem unlikely that clusters with comparable ages could have substantially different $[\text{Ca}/\text{Fe}]$ ratios. Thus the difference in W' between Lindsay 11 and NGC 339, for example, is likely to reflect a significant difference in overall abundance.

The final issue is that of the calibration relation itself. As noted above, in DA95 the W' calibration is tied to the globular cluster abundance scale of Zinn & West (1984). In a recent paper, however, Carretta & Gratton (1997) have compiled a consistent set of $[\text{Fe}/\text{H}]$ values derived from high dispersion spectroscopy for galactic globular clusters. These authors find that their $[\text{Fe}/\text{H}]$ values do not scale linearly with those of Zinn & West (1984). While there is reasonable agreement for both the metal-poor ($[\text{Fe}/\text{H}] \approx -2.0$) and the metal-rich ($[\text{Fe}/\text{H}] \approx -0.7$) clusters, at intermediate abundances there are substantial differences (Carretta & Gratton 1997). For example, the “standard clusters” M3, M13 and M5 have abundances on the Zinn & West (1984) scale of -1.66 , -1.65 and -1.40 dex but have $[\text{Fe}/\text{H}]_{\text{CG97}} = -1.34$, -1.39 and -1.11 , respectively, a difference of a factor of 2 in Z .

Further, Rutledge *et al.* (1997) have shown that the non-linear relation between W' and $[\text{Fe}/\text{H}]_{\text{ZW84}}$ becomes linear when $[\text{Fe}/\text{H}]_{\text{CG97}}$ is used instead. This is illustrated in Fig. 3 where we plot the W' values for the calibration clusters in Table 4 of DA95 against $[\text{Fe}/\text{H}]_{\text{CG97}}$. A single straight line fits the data over the entire $[\text{Fe}/\text{H}]_{\text{CG97}}$ abundance range (cf. Rutledge *et al.* 1997). A least squares fit to these data then yields:

$$[\text{Fe}/\text{H}]_{\text{CG97}} = (0.416 \pm 0.018)W' - (2.748 \pm 0.064) \quad (2)$$

The rms deviation in $[\text{Fe}/\text{H}]_{\text{CG97}}$ about the fitted line is 0.07 dex. Rutledge *et al.* (1997) find a very similar relation. Fig. 3 also shows the two segment calibration relation of DA95 for comparison. At the moment it is not obvious which abundance scale is correct though the high dispersion studies of Sneden, Kraft and co-workers (e.g., Kraft *et al.* 1995 and references therein), for example, do support the Carretta & Gratton (1997) results for the clusters in common.

With the exception of Lindsay 11, all the observed SMC cluster W' values fall in the range where the $(W', [\text{Fe}/\text{H}]_{\text{ZW84}})$ and $(W', [\text{Fe}/\text{H}]_{\text{CG97}})$ calibrations differ significantly. Thus we will interpret our results using both calibration relations. In Table 3 then, we list 4 abundances for each SMC cluster. These are abundances with and without the correction for the brightening of

the horizontal branch with decreasing age, and for both the $[\text{Fe}/\text{H}]_{\text{ZW84}}$ calibration of DA95 and the $[\text{Fe}/\text{H}]_{\text{CG97}}$ derived above. The errors listed include both the uncertainty in the W' value from Table 2 and the uncertainty in the particular calibration. These uncertainties are comparable in size for clusters such as Lindsay 113, but for clusters with smaller errors in W' , such as NGC 339, the calibration error dominates. In general, the results in Table 3 reveal no major surprises: the abundances are not very different (though of higher precision) from existing estimates based on integrated spectroscopy and photometry and/or red giant branch colors. For example, Zinn & West (1984) list $[\text{Fe}/\text{H}] = -1.51 \pm 0.15$ for NGC 121 in excellent agreement with our value of $[\text{Fe}/\text{H}]_{\text{ZW84}} = -1.46 \pm 0.10$ dex.

4. Results

4.1. Kinematics of the Cluster Sample

The analysis of the kinematics of the cluster system of the LMC has revealed generally ordered motion. For example, the majority of the clusters form a disk system whose parameters agree with those of the optical isophotes and the H I rotation curve (Schommer *et al.* 1992). Further, unlike the at most slowly rotating, pressure supported, galactic halo globular cluster system, even the oldest LMC star clusters have the kinematics of a disk system: the rotation amplitude is comparable to that of the younger clusters and the velocity dispersion is relatively small (Schommer *et al.* 1992). For the SMC, however, the situation is apparently quite different. Kinematic studies of both planetary nebula (Dopita *et al.* 1985) and carbon star (Hardy *et al.* 1989, Hatzidimitriou *et al.* 1997) samples have not revealed any indications of systematic rotation, while the recent high resolution study of the H I in the SMC reveals a complex structure dominated by the effects of expanding H I shells, rather than a rotating disk-like structure (Stavely-Smith *et al.* 1997). The on-going interaction with the LMC (and with the Galaxy) undoubtedly also influences the kinematics of SMC populations, particularly in the outer regions to north-east of the SMC center and in the Wing (e.g., Hatzidimitriou *et al.* 1993).

While our sample of intermediate-age and old SMC star clusters is small, it is nevertheless distributed over the entire spatial extent of the SMC. Thus it is worthwhile investigating the kinematics implied by the cluster radial velocities. Moreover, the ages of the star clusters studied range from ~ 4 to ~ 12 Gyr and thus it is sensible to compare the cluster results with those from the planetary nebula (Dopita *et al.* 1985) and carbon star (Hardy *et al.* 1989, Hatzidimitriou *et al.* 1997) samples. Both these populations have progenitors whose ages are comparable to those of the star clusters. Also available for comparison is the study of the kinematics of SMC red clump stars (Hatzidimitriou *et al.* 1993) and that for SMC field red giants (Suntzeff *et al.* 1986). These studies are restricted to particular areas; a region near NGC 121 in the latter case and a region approximately 3.5° north-east of the SMC center in the former case.

As mentioned above, both the planetary nebula and the carbon star samples show no evidence

for any systematic rotation of the SMC, and our cluster velocities support this conclusion. In particular, the seven clusters fall within the scatter shown by the carbon stars in the (V_{GSR} , position angle) diagram of Hardy *et al.* (1989). Similarly, in the (V_{GSR} , projected distance from the centroid along the SMC major axis) diagram of Dopita *et al.* (1985), the clusters are indistinguishable from the planetary nebulae. We have then used a maximum likelihood code kindly provided by Tad Pyror to calculate the mean velocity $\langle V_r \rangle$ and velocity dispersion σ for the cluster sample³. The results are, using heliocentric values, $\langle V_r \rangle = 138 \pm 6 \text{ km s}^{-1}$ and $\sigma = 16 \pm 4 \text{ km s}^{-1}$. The results are summarized and compared with other samples in Table 4. The mean velocity of the cluster sample is in good accord with those for the other samples. The dispersion though, is somewhat lower: $16 \pm 4 \text{ km s}^{-1}$ versus $21 - 27 \text{ km s}^{-1}$ for the other large area surveys. Given the small number of clusters in our sample we ascribe no significance to this difference. It is interesting to note though that the dispersion of the old and intermediate-age populations in the SMC is, at $\sim 24 \text{ km s}^{-1}$, very comparable to the dispersion seen for the LMC clusters of similar age (Schommer *et al.* 1992). The major kinematic difference though lies in the substantial rotation of the LMC cluster system ($V_{\text{circ}} \gtrsim 50 \text{ km s}^{-1}$) which is apparently completely lacking in the SMC. It is of further interest to note that Staveland-Smith *et al.* (1997) also find a similar dispersion ($25 \pm 0.6 \text{ km s}^{-1}$) from their SMC H I observations. When combined with, for example, the Cepheid observations of Mathewson *et al.* (1988) for which $\sigma = 22 \pm 3 \text{ km s}^{-1}$, it is evident that the kinematics of the various SMC populations studied are all similar. As a result, it appears that kinematics are independent of age in the SMC. This result contrasts rather strongly with the situation in our Galaxy and in the LMC, but whether it is a result of the interaction history of the SMC remains unclear.

4.2. The SMC Age-Metallicity Relation

In Table 2 we list our adopted ages for the six clusters in our sample for which we have determined metallicities. These ages have generally been taken from the original *c-m* diagram references (cf. Sect. 2.1) and are appropriate for our assumed SMC distance modulus of $(m-M)_0 = 18.8$. For Kron 3, however, we have taken account of the results of Alcaino *et al.* (1996) who found a somewhat older age than did Rich *et al.* (1984). Similarly, for Lindsay 113, we follow Seidel *et al.* (1987a) who noted that the apparent magnitude of the red clump in this cluster, which lies at the extreme eastern edge of the SMC, suggests that it is $\sim 0.2 - 0.3 \text{ mag}$ closer than the standard SMC modulus. Consequently, we have adopted the Seidel *et al.* (1987a) value of $6 \pm 1 \text{ Gyr}$ for the age of this cluster rather than the somewhat younger value given by Mould *et al.* (1984). In all cases we have assigned relatively generous error bars to the adopted ages. Fig. 4 plots our spectroscopic abundance determinations for these six clusters against the adopted ages.

³For this sample, the maximum likelihood analysis gives essentially identical results to those generated by applying the formalism of Armandroff & Da Costa (1986).

The upper panel shows the abundances on the Zinn & West (1984) scale while the lower panel employs the Carretta & Gratton (1997) abundance scale. In both panels the abundance plotted is that corrected for the variation with age of the horizontal branch luminosity (cf. Table 3).

In Fig. 4 we have also plotted additional data relevant to defining the age-metallicity relation of the SMC. We now briefly discuss these data. First, in Fig. 4 points are plotted for five additional clusters: NGC 152, NGC 330, NGC 411, NGC 419 and NGC 458. For NGC 152 the abundance ($[\text{Fe}/\text{H}] = -0.8 \pm 0.3$) is from Hodge (1981a) and is based on the giant branch color. The adopted age of 1.9 ± 0.5 Gyr comes from considering the magnitude difference between the main sequence turnoff and the red clump in the c-m diagram of Hodge (1981b); see Mould & Da Costa (1988) for details. For NGC 411 we adopted the age (1.8 ± 0.3 Gyr) given by Da Costa & Mould (1986) for our adopted SMC modulus. The abundance for this cluster ($[\text{Fe}/\text{H}] = -0.84 \pm 0.3$ dex) also comes from the giant branch color: Da Costa & Mould (1986) determine an abundance of -0.6 ± 0.3 dex relative to the galactic cluster NGC 7789 for which Friel (1995) lists $[\text{Fe}/\text{H}] = -0.24$ dex. The age (1.2 ± 0.5 Gyr) and abundance ($[\text{Fe}/\text{H}] = -0.7 \pm 0.3$) adopted for NGC 419 follow from the c-m diagram isochrone fits of Durand *et al.* (1984) who also indicate that integrated Washington system photometry of this cluster requires $[\text{Fe}/\text{H}] \gtrsim -1.0$ dex. These results are consistent with those of Rabin (1983) who showed from integrated spectra that NGC 419 and NGC 411 occupy essentially identical locations in a (hydrogen line strength, calcium K line strength) diagram. For NGC 458, Papenhausen & Schommer (1988) list an age of 0.3 Gyr based on fitting a $\log(Z/Z_{\odot}) = -0.23$ isochrone from Vandenberg (1985). Given the uncertainty of abundance determination via isochrone fits, we have in this case adopted a larger error for the abundance. In particular, the adopted error covers the comment of Stothers & Chin (1992) that NGC 458 is likely to have an abundance similar to that of the average SMC young population. Our adopted age error of ± 0.2 Gyr also encompasses the Stothers & Chin (1992) age estimate of ~ 0.1 Gyr for this cluster. Finally, we adopt an abundance of $[\text{Fe}/\text{H}] = -0.82 \pm 0.10$ for the young (age = 0.025 ± 0.015 Gyr, Choisi *et al.* 1995) cluster NGC 330. This abundance is from the high dispersion spectroscopic study of Hill & Spite (1997, see also Meliani *et al.* 1995 and the references therein).

Figure 4 also includes relevant data for SMC field objects. In particular, we have plotted, at an adopted age of 13 ± 1 Gyr, the mean abundance found by Butler *et al.* (1982) for 7 SMC RR Lyrae stars in a field near NGC 121. Further, Suntzeff *et al.* (1986) have studied both spectroscopically and photometrically a proper motion selected sample of ~ 30 SMC red giants, again in a field near NGC 121. The mean abundance of these stars is $[\text{Fe}/\text{H}] = -1.56 \pm 0.06$ and a real abundance spread is apparently present in these data. Fig. 9 of Suntzeff *et al.* (1986) suggests a total abundance range from perhaps $[\text{Fe}/\text{H}] \approx -2.1$ to $[\text{Fe}/\text{H}] \approx -1.2$. Here it is relevant to note that the Suntzeff *et al.* (1986) results are on the Zinn & West (1984) scale and that both the upper limit on the abundance distribution and the mean abundance would be raised if the Carretta & Gratton (1997) scale was used instead. However, of all the additional results presented in Fig. 4, these are the only ones affected by the abundance scale difference. As for the likely ages of the stars in the Suntzeff *et al.* (1986) sample, individual determinations are, of course, not possible

but we can turn to the field region results of Stryker *et al.* (1985). These authors find that the field population near NGC 121 is dominated by old stars (unlike the LMC) and they suggest an age range from perhaps 8 to 14 Gyr is present. The actual age distribution, however, is unknown.

Finally, we also show in Fig. 4 representative values of the present-day abundance in the SMC. These determinations are from the high dispersion spectroscopic studies of Russell & Bessell (1989), $[\text{Fe}/\text{H}] = -0.65 \pm 0.06$ from 8 F-type supergiants, Luck & Lambert (1992), $[\text{Fe}/\text{H}] = -0.53 \pm 0.05$ from 7 Cepheids and supergiants, and Hill (1997), $[\text{Fe}/\text{H}] = -0.69 \pm 0.05$ from 6 K-type supergiants. These studies are consistent with each other and none provide any compelling evidence for the existence of any substantial abundance range among the youngest populations in the SMC. Russell & Dopita (1990) also find no significant metallicity spread among the H II regions of the SMC, in agreement with the earlier result of Pagel *et al.* (1978).

5. Discussion

The appearance of the SMC age-metallicity relation in Fig. 4 is somewhat different from previous depictions of the cluster and field star data (e.g., Stryker *et al.* 1985, Da Costa 1991, Olszewski *et al.* 1996) principally as a result of the increased precision of our spectroscopic abundance determinations. Leaving aside for the moment the two clusters (Lindsay 113 and NGC 339) with anomalously low abundances, the enrichment history for the SMC indicated by Fig. 4 suggests a relatively rapid ($\tau \lesssim 3$ Gyr) initial abundance increase followed by a more modest rise starting at ~ 10 Gyr and continuing until the present day. In particular, the previous requirement (e.g., Da Costa 1991) for an increased rate of enrichment to bring the abundance from $[\text{Fe}/\text{H}] \approx -1.3$ at approximately 3 Gyr to the present-day value of $[\text{Fe}/\text{H}] \approx -0.6$ is alleviated. Indeed, the data of Fig. 4, again excepting Lindsay 113 and NGC 339, are now quite consistent with the predictions of the simple “closed box” model of chemical evolution. Thus it is also no longer necessary to postulate the significant gas infall or strong galactic winds which were invoked (e.g., Dopita 1991) to explain the apparent lack of enrichment from $\sim 10 - 12$ Gyr to approximately 3 Gyr. Of course such processes, however, may still take place.

The SMC, with its likely past interactions with the LMC and the Galaxy may well be an “open” rather than a closed box, but nevertheless simple models scaled to a present-day abundance, the current SMC gas mass fraction (taken as 0.36, Lequeux 1984) and a formation epoch, assumed to be at 15 Gyr, give reasonable representations of the data. This is especially the case in the upper panel of Fig. 4 where we show simple models with present-day abundances of $\log Z/Z_{\odot} = -0.6$ and $\log Z/Z_{\odot} = -0.5$ dex. The scatter about the model curves is entirely consistent with the uncertainties in the data. In the lower panel of Fig. 4 the same simple model curves are shown. Here the fit is somewhat less satisfactory: the rate of enrichment from ~ 10 Gyr to the present suggested by the observations being generally somewhat lower than the model predictions. Or conversely, the rate of enrichment prior to ~ 10 Gyr may have been more rapid than the simple model predicts. The model fits to the data in the lower panel of Fig. 4 could no

doubt be improved by invoking infall, for example, but tighter constraints on the age-metallicity relation are required before such additional calculations would be meaningful.

We now turn to the “anomalous” clusters Lindsay 113 and NGC 339. These clusters have abundances approximately 0.5 and 0.65 dex lower, respectively, than the simple model curves predict for their ages on the Zinn & West (1984) abundance scale, or ~ 0.25 and 0.4 dex lower, respectively, using the Carretta & Gratton (1997) scale⁴. These clusters are considered anomalous since in dwarf galaxies like the SMC, provided the star formation rate is relatively constant and the infall of external material insignificant, the expanding gas shells driven by evolving massive stars should thoroughly mix the interstellar medium over galaxy-wide scales on timescales that are considerably less than a Hubble time (e.g., Roy & Kunth 1995, see also Kobulnicky & Skillman 1997). At the present epoch it does appear that the SMC is chemically homogeneous. The studies listed above indicate that for both the young field stars and the H II regions the maximum abundance dispersion permitted by the observations is $\lesssim 0.1$ dex. Further, while there has been considerable controversy in the past regarding the abundance of the young massive star cluster NGC 330, recent work (e.g., Hill & Spite 1997) suggests that this cluster is only ~ 0.1 dex more metal-poor than field objects of comparable age, a minor offset. As regards the LMC, where there is a large population of intermediate-age star clusters, we can draw on the results of Olszewski *et al.* (1991) who also used Ca II triplet spectroscopy to determine abundances for a large number of LMC star clusters. Olszewski *et al.* (1991) indicate that for the clusters in the age range 0.5 to 3 Gyr, the inner ($r < 5^\circ$ or ~ 4 kpc) and outer clusters have “apparently the same abundance spread, both of which are consistent with the measurement errors (in) our metallicities” (Olszewski *et al.* 1991). Thus there is no compelling case for a significant abundance spread among the LMC intermediate-age clusters. However, in the Olszewski *et al.* (1991) sample, one can find relatively well observed clusters such as Hodge 14 (5 observations of 3 stars, $[\text{Fe}/\text{H}] = -0.66$) and NGC 1777 (3 observations of 3 stars, $[\text{Fe}/\text{H}] = -0.35$) for which the results do suggest the existence of an intrinsic abundance range among the intermediate-age LMC clusters of size perhaps $\lesssim 0.3$ dex. But this abundance range is considerably less than that between the SMC clusters NGC 339 and Lindsay 11 ($\Delta[\text{Fe}/\text{H}] = 0.66 \pm 0.17$ on the Zinn & West (1984) abundance scale, which is that used by Olszewski *et al.* 1991; $\Delta[\text{Fe}/\text{H}] = 0.38 \pm 0.16$ on the Carretta & Gratton 1997 scale), again pointing to the unusual nature of the two SMC low abundance clusters. Indeed these abundance differences are comparable in size to the *full range* in abundance seen in the galactic disk age-metallicity relation at comparable age (Edvardsson *et al.* 1993).

⁴In this latter case it could be argued that Lindsay 113 lies below the model curve for a present-day abundance of -0.6 dex by an amount comparable to which clusters such as Lindsay 1 and Kron 3 lie above it. Thus Lindsay 113 would not be anomalous but would instead be a reflection of an intrinsic abundance range of ~ 0.2 dex present in the SMC over at least the 5 – 10 Gyr epoch. If it were not for NGC 339, which lies further below the model line and which has an abundance difference of ~ 0.4 dex on the Carretta & Gratton (1997) scale from the similar aged cluster Lindsay 11, such an interpretation might be plausible. However, we prefer to work on the assumption that the bulk of the SMC population at any age less than ~ 10 Gyr has only a small abundance range, and that therefore these two clusters are anomalous. Additional data will, of course, eventually validate or refute this interpretation.

Can we then offer an explanation for their anomalously low abundances? We note first that Lindsay 113 lies in the extreme eastern part of the SMC some 4.2° (~ 4.2 kpc in projection) from the center, while NGC 339 lies 1.5° to the south. This might suggest an abundance gradient but in fact all the other clusters in our abundance sample are further from the SMC center, at least in projection, than NGC 339. In particular, Lindsay 1 lies 3.4° to the west and does not appear anomalous. We can also use the age-compensated horizontal branch magnitudes to investigate any possible line-of-sight distance variations. These data suggest that Kron 3, Lindsay 11, NGC 121 and NGC 339 are at approximately the same distance, while Lindsay 1 and Lindsay 113 are perhaps ~ 0.3 mag closer. Again it seems that a simple abundance gradient is not the answer.

As for other explanations, a number of possibilities exist. Roy & Kunth (1995), for example, suggest that large abundance discontinuities might arise in dwarf galaxies lacking significant differential rotation if there are long dormant phases between successive star forming episodes. This might appear an attractive possibility given the SMC’s apparent lack of rotation, but the existence of a relatively uniform age distribution for the SMC star clusters with main sequence turnoff age determinations (cf. Fig. 4) argues against the required long dormant phases.

The remaining possibility is that the formation of these clusters involves the infall of unenriched, or at least less enriched, gas⁵. Given the extensive H I halo surrounding both Magellanic Clouds (e.g., Mathewson & Ford, 1984) and the existence of the Magellanic Stream, this possibility seems plausible. We note, however, that Lu *et al.* (1994) have used absorption line spectroscopy of a background source to argue that the Magellanic Stream gas is certainly not of primordial ($\log Z/Z_\odot \lesssim -2$) composition. Indeed the abundance limits are consistent with present-day Magellanic Cloud abundances (Lu *et al.* 1994). If these abundances are generally applicable to the Magellanic Stream gas, then it would seem to rule out the Magellanic Stream as the source of the low abundance gas involved in the formation of these clusters. However, Lu *et al.* (1994) caution that the greatest uncertainty in abundance studies of this type is the sampling differences that can result from the narrow pencil beam of the absorption line data versus the large beam of the 21cm data. Since the H I column density can vary substantially on small scales (cf. the high resolution SMC H I map of Staveley-Smith *et al.* 1997 versus the earlier Parkes data of, for example, Mathewson & Ford 1984), the true abundances could differ substantially from the derived values. We note also that postulating a Magellanic Stream origin for the low abundance gas involved in the formation of these clusters requires that the Stream have an age of at least 4 Gyr. This conflicts with at least some models for the Stream’s origin (e.g., Gardiner & Noguchi 1996).

A further speculative possibility is that the gas from which Lindsay 113 and NGC 339

⁵We postulate that the gas from which these clusters formed consists of a mixture of SMC gas with the abundance “expected” for the cluster ages, diluted by a component with a lower abundance. Given that these clusters have abundances Z approximately a factor of 3 lower than expected from the simple model curves, the required dilution factors range from 0.67 for unenriched gas to 1.00 for gas with abundance equal to that of the clusters.

formed (presumably separately since the clusters have different ages) contained a low abundance component which had been expelled in galactic wind at an early epoch, but which remained bound to the SMC and which subsequently cooled and fell back (cf. Tenorio-Tagle 1996, Burkert & Ruiz-Lapuente 1997). A second speculative possibility is that the SMC acquired these clusters in a past interaction much in the same way that the Galaxy is now acquiring clusters from the Sagittarius dwarf galaxy (e.g., DA95). However, we note that among the dwarf galaxies of the Local Group, the only system known to contain star clusters of age similar to Lindsay 113 and NGC 339 (i.e., $\sim 4 - 6$ Gyr) is the SMC itself!

We conclude by noting that the chemical evolution of the SMC, as exhibited by the data described here for old and intermediate-age clusters, is obviously quite complex. If we are to provide further constraints on the processes involved, then it is necessary to determine abundances (and ages) for additional SMC star clusters. There are a number of candidate clusters (e.g., NGC 361) whose ages are likely to lie between 1 to 2 Gyr and ~ 10 Gyr. The results for such clusters would help enormously in clarifying whether the low abundances exhibited by Lindsay 113 and NGC 339 are common, or are restricted to only a small fraction of SMC cluster population. There are no technical difficulties preventing the collection of such data.

The authors wish to thank Dr. Taft Armandroff for reducing some of the spectra used in this paper and Dr. Tad Pyror for a copy of his maximum likelihood velocity dispersion code. We are also grateful to Dr. Ed Olszewski for supplying details of his study of NGC 339 in advance of publication and to an anonymous referee for helpful comments. The AAT staff also deserve our thanks for support at the telescope.

REFERENCES

- Alcaino, G., Liller, W., Alvarado, F., Kravtsov, V., Ipatov, A., Samus, N., & Smirnov, O. 1996, *AJ*, 112, 2004
- Armandroff, T.E., & Da Costa, G.S. 1986, *AJ*, 92, 777
- Armandroff, T.E., & Da Costa, G.S. 1991, *AJ*, 101, 1329
- Arp, H.C. 1958, *AJ*, 63, 487
- Bertelli, G., Bressan, A., Chiosi, C., Fagotto, F., & Nasi, E. 1994, *A&AS*, 106, 275
- Bulter, D., Demarque, P., & Smith, H.A. 1982, *ApJ*, 257, 592
- Burkert, A., & Ruiz-Lapuente, P. 1997, *ApJ*, 480, 297
- Carretta, E., & Gratton, R.G. 1997, *A&AS*, 121, 95
- Choi, C., Vallenari, A., Bressan, A., Deng, L., & Ortolani, S. 1995, *A&A*, 293, 710
- Da Costa, G.S. 1991, in *The Magellanic Clouds*, IAU Symposium 148, edited by R. Haynes and D. Milne (Kluwer, Dordrecht), p. 183

- Da Costa, G.S., & Armandroff, T.E. 1995, *AJ*, 109, 2533 (DA95)
- Da Costa, G.S., & Mould, J.R. 1986, *ApJ*, 305, 214
- Dopita, M.A. 1991, in *The Magellanic Clouds*, IAU Symposium 148, edited by R. Haynes and D. Milne (Kluwer, Dordrecht), p. 393
- Dopita, M.A., Ford, H.C., Lawrence, C.J., & Webster, B.L. 1985, *ApJ*, 296, 390
- Dubath, P., Meylan, G., & Mayor, M. 1997, *A&A*, 324, 505
- Durand, D., Hardy, E., & Melnick, J. 1984, *ApJ*, 283, 552
- Edvardsson, B., Andersen, J., Gustafsson, B., Lambert, D.L., Nissen, P.E., & Tomkin, J. 1993, *A&A*, 275, 101
- Friel, E.D. 1995, *ARA&A*, 33, 381
- Gardiner, L.T., & Noguchi, M. 1996, *MNRAS*, 278, 191
- Gascoigne, S.C.B. 1980, in *Star Clusters*, IAU Symposium 85, edited by J.E. Hesser (Reidel, Dordrecht), p. 305
- Geisler, D., Bica, E., Dottori, H., Claria, J.J., Piatti, A.E., & Santos, J.F.C. Jr. 1997, *AJ*, 114, 1920
- Green, E.M., Demarque, P., & King, C.R. 1987, *The Revised Yale Isochrones and Luminosity Functions* (Yale Univ. Obs., New Haven)
- Hardy, E., Suntzeff, N.B., & Azzopardi, M. 1989, *ApJ*, 344, 210
- Hatzidimitriou, D. 1991, *MNRAS*, 251, 545
- Hatzidimitriou, D., Cannon, R.D., & Hawkins, M.R.S. 1993, *MNRAS*, 261, 873
- Hatzidimitriou, D., Croke, B.F., Morgan, D.H., & Cannon, R.D. 1997, *A&AS*, 122, 507
- Hesser, J.E., Shawl, S.J., & Meyer, J.E. 1986, *PASP*, 98, 403
- Hill, V. 1997, *A&A*, 324, 435
- Hill, V., & Spite, M. 1997, in *Cosmic Chemical Evolution*, IAU Symposium 187, edited by J.W. Truran and K. Nomoto (Kluwer, Dordrecht), in press
- Hodge, P. 1981a, in *Astrophysical Parameters for Globular clusters*, IAU Colloquium 68, edited by A.G.D. Philip and D.S. Hayes (L. Davis Press, Schenectady), p. 205
- Hodge, P.W. 1981b, *ApJ*, 247, 894
- Kobulnicky, H.A., & Skillman, E.D. 1997, *ApJ*, 489, 636
- Kraft, R.P., Sneden, C., Langer, G.E., Shetrone, M.D., & Bolte, M. 1995, *AJ*, 109, 2586
- Lequeux, J. 1984, in *Structure and Evolution of the Magellanic Clouds*, IAU Symposium 108, edited by S. van den Bergh and K.S. de Boer (Reidel, Dordrecht), p. 67
- Lu, L, Savage, B.D., & Sembach, K.R. 1994, *ApJ*, 437, L119

- Luck, R.E., & Lambert, D.L. 1992, *ApJS*, 79, 303
- Mateo, M., Hodge, P., & Schommer, R.A. 1986, *ApJ*, 311, 113
- Mathewson, D.S., & Ford, V.L. 1984, in *Structure and Evolution of the Magellanic Clouds*, IAU Symposium 108, edited by S. van den Bergh and K.S. de Boer (Reidel, Dordrecht), p. 125
- Mathewson, D.S., Ford, V.L., & Visvanathan, N. 1988, *ApJ*, 333, 617
- Meliani, M.T., Barbuy, B., & Perrin, M.-N. 1995, *A&A*, 300, 349
- Mould, J., & Aaronson, M. 1982, *ApJ*, 263, 629
- Mould, J.R., & Da Costa, G.S. 1988, in *Progress and Opportunities in Southern Hemisphere Optical Astronomy*, ASP Conf. Ser., Vol. 1, edited by V.M. Blanco and M.M. Phillips (A.S.P., San Francisco), p. 197
- Mould, J.R., Da Costa, G.S., & Crawford, M.D. 1984, *ApJ*, 280, 595
- Mould, J.R., Jensen, J.B., & Da Costa, G.S. 1992, *ApJS*, 82, 489
- Olszewski, E.W., Schommer, R.A., & Aaronson, M. 1987, *AJ*, 93, 565
- Olszewski, E.W., Schommer, R.A., Suntzeff, N.B., & Harris, H.C. 1991, *AJ*, 101, 515
- Olszewski, E.W., Suntzeff, N.B., & Mateo, M. 1996, *ARA&A*, 34, 511
- Pagel, B.E.J., Edmunds, M.G., Fosbury, R.A.E., & Webster, B.L. 1978, *MNRAS*, 184, 569
- Pagel, B.E.J., & Tautvaisiene, G. 1995, *MNRAS*, 276, 505
- Papenhause, P., & Schommer, R.A. 1988, in *The Harlow Shapley Symposium on Globular Cluster Systems in Galaxies*, IAU Symposium 126, edited by J.E. Grindlay and A.G.D. Philip (Kluwer, Dordrecht), p. 565
- Rabin, D. 1983, *ApJ*, 261, 85
- Rich, R.M., Da Costa, G.S., & Mould, J.R. 1984, *ApJ*, 286, 517
- Roy, J.-R., & Kunth, D. 1994, *A&A*, 294, 432
- Russell, S.C., & Bessell, M.S. 1989, *ApJS*, 70, 865
- Russell, S.C., & Dopita, M.A. 1990, *ApJS*, 74, 93
- Rutledge, G.A., Hesser, J.E., & Stetson, P.B. 1997, *PASP*, 109, 907
- Schommer, R.A., Olszewski, E.W., Suntzeff, N.B., & Harris, H.C. 1992, *AJ*, 103, 447
- Seidel, E., Da Costa, G.S., & Demarque, P. 1987a, *ApJ*, 313, 192
- Seidel, E., Demarque, P., & Weinberg, D. 1987b, *ApJS*, 63, 917
- Staveley-Smith, L., Sault, R.J., Hatzidimitriou, D., Kesteven, M.J., & McConnell, D. 1997, *MNRAS*, 289, 225
- Stothers, R.B., & Chin. C.-W. 1992, *ApJ*, 390, 136
- Stryker, L.L., Da Costa, G.S., & Mould, J.R. 1985, *ApJ*, 298, 544

- Suntzeff, N.B., Friel, E., Klemola, A., Kraft, R.P., & Graham, J.A. 1986, *AJ*, 91, 275
- Suntzeff, N.B., Schommer, R.A., Olszewski, E.W., & Walker, A.R. 1992, *AJ*, 104, 1743
- Tenorio-Tagle, G. 1996, *AJ*, 111, 1641
- Tift, W.G. 1963, *MNRAS*, 125, 199
- VandenBerg, D.A. 1985, *ApJS*, 58, 711
- van den Bergh, S. 1981, *A&AS*, 46, 79
- Wheeler, J.C., Sneden, C., & Truran, J.W.Jr. 1989, *ARA&A*, 27, 279
- Zinn, R., & West, M.J. 1984, *ApJS*, 55, 45

Table 1. Data for Program Cluster Stars

Cluster	Star	V	$B - V$	$W_{8542} + W_{8862}(\text{\AA})$	Notes
Lindsay 1	OSA783	17.01	1.37	5.76 ± 0.28	1
	OAS426	17.02	1.39	5.38 ± 0.22	1
	OAS453	17.06	1.36	5.41 ± 0.25	1
	OAS772	17.11	1.38	5.67 ± 0.32	1
Kron 3	RDM406	16.69	1.51	6.23 ± 0.42	2
	RDM408	16.80	1.45	5.86 ± 0.41	2
	RDM303	16.83	1.44	6.01 ± 0.33	2
	RDM099	17.25	1.28	5.39 ± 0.43	2
Lindsay 11	MJD182	16.86	1.56	6.38 ± 0.33	2
	MJD240	16.95	1.47	5.03 ± 0.23	1,2,3
	MJD177	17.19	1.33	6.42 ± 0.40	2
	MJD192	17.52	1.28	5.78 ± 0.29	1,2
	MJD233	18.12	0.98	5.67 ± 0.53	2,4
	MJD212	18.15	1.16	6.33 ± 0.52	2,4
NGC 121	SDM029	17.03	1.40	4.71 ± 0.33	2,5
	SDM063	17.34	1.34	4.74 ± 0.44	2,4
	SDM123	18.04	1.09	4.43 ± 0.44	2,4
	SDM132	18.06	1.14	4.55 ± 0.32	2,4
	SDM193	18.12	1.16	5.01 ± 0.27	2,4
NGC 339	OAS171	17.14	1.35	5.30 ± 0.22	1
	OAS392	17.14	1.39	5.52 ± 0.31	1
	OAS126	17.16	1.33	5.32 ± 0.28	1
	OAS226	17.20	1.18	5.15 ± 0.23	1
	OAS429	17.29	1.24	5.17 ± 0.30	1
	OAS104	17.30	1.23	4.99 ± 0.27	1
NGC 361	Arp I-15	16.4	1.4	6.08 ± 0.32	...
	Arp I-35	16.5	1.4	5.82 ± 0.33	...
	Arp I-51	16.7	1.4	6.20 ± 0.28	1
	Arp I-63	16.8	1.2	5.45 ± 0.30	1

Table 1—Continued

Cluster	Star	V	$B - V$	$W_{8542} + W_{8862}(\text{\AA})$	Notes
Lindsay 113	MDC280	16.96	1.32	5.20 ± 0.36	2
	MDC098	17.03	1.28	6.28 ± 0.62	2
	MDC281	17.04	1.17	5.28 ± 0.26	2,6
	MDC078	17.21	1.23	4.42 ± 0.44	2,4

Note. — (1) Listed $W_{8542} + W_{8862}$ value is the mean from two spectra. (2) V , $B - V$ values derived from R , $B - R$ photometry. (3) Line strength discrepant: not a cluster member but radial velocity indicates SMC membership. (4) Listed $W_{8542} + W_{8862}$ value is from summed spectra. (5) Radial velocity indicates Galactic foreground star. (6) Listed $W_{8542} + W_{8862}$ value is the mean from three spectra.

Identification and Photometry Sources: Lindsay 1, Olszewski *et al.* (1987); Kron 3, Rich *et al.* (1984); Lindsay 11, Mould *et al.* (1992); NGC 121, Stryker *et al.* (1985); NGC 339, Olszewski (priv. comm.); NGC 361, Arp (1958); Lindsay 113, Mould *et al.* (1984). Except for the photographic data of Arp (1958), all photometry is derived from CCD images.

Table 2. SMC Cluster Observed Data

Cluster	Age (Gyr)	V_{HB}	W' (\AA)	V_r (km s^{-1})	N
Lindsay 1	10 \pm 2	19.20	4.22 \pm 0.11	126 \pm 3	4
Kron 3	9 \pm 2	19.44	4.29 \pm 0.14	123 \pm 3	4
Lindsay 11	3.5 \pm 1	19.50	4.81 \pm 0.18	132 \pm 5	5
NGC 121	12 \pm 2	19.60	3.74 \pm 0.18	138 \pm 4	4
NGC 339	4 \pm 1.5	19.36	3.91 \pm 0.07	117 \pm 8	6
NGC 361	164 \pm 6	4
Lindsay 113	6 \pm 1	19.13	3.91 \pm 0.19	162 \pm 4	4

Table 3. SMC Cluster Abundance Results

Cluster	$[\text{Fe}/\text{H}]_{\text{ZW84}}$		$[\text{Fe}/\text{H}]_{\text{CG97}}$	
	Raw	$V_{HB}(\text{age})_{\text{corrected}}$	Raw	$V_{HB}(\text{age})_{\text{corrected}}$
Lindsay 1	-1.14 ± 0.10	-1.17 ± 0.10	-0.99 ± 0.11	-1.01 ± 0.11
Kron 3	-1.08 ± 0.12	-1.12 ± 0.12	-0.96 ± 0.12	-0.98 ± 0.12
Lindsay 11	-0.70 ± 0.14	-0.80 ± 0.14	-0.75 ± 0.13	-0.81 ± 0.13
NGC 121	-1.46 ± 0.10	-1.46 ± 0.10	-1.19 ± 0.12	-1.19 ± 0.12
NGC 339	-1.36 ± 0.10	-1.46 ± 0.10	-1.12 ± 0.10	-1.19 ± 0.10
Lindsay 113	-1.37 ± 0.16	-1.44 ± 0.16	-1.12 ± 0.12	-1.17 ± 0.12

Table 4. Kinematics of SMC Old and Intermediate-Age Populations

Sample	N	$\langle V_r \rangle_{helio}$ (km s ⁻¹)	$\langle V_r \rangle_{LSR}$ (km s ⁻¹)	Dispersion (km s ⁻¹)	Ref
Star Clusters	7	138 ± 6	127 ± 6	16 ± 4	1
Planetary Nebulae	44	...	134 ± 4	25 ± 3	2
Carbon Stars ^a	131	148 ± 2	140 ± 2	27 ± 2	3
Carbon Stars ^b	62	146 ± 3	...	21 ± 2	4
Red Clump Stars ^c	29	151 ± 6	...	33 ± 4 ^d	5
Red Giants ^e	12	123 ± 7	...	18 ± 5 ^f	6

^aCentral Region of SMC only

^bPrincipally Outer Regions of SMC, Outer Wing excluded

^c40' diameter region 3.5° north-east of the SMC center

^dDispersion is ~18 km s⁻¹ after correction for velocity, distance correlation

^eNear NGC 121 only

^fValue is that corrected for observed velocity errors

Note. — *References:* (1) This paper, (2) Dopita *et al.* (1985), (3) Hardy *et al.* (1989), (4) Hatzidimitriou *et al.* (1997), (5) Hatzidimitriou *et al.* (1993), (6) Suntzeff *et al.* (1986).

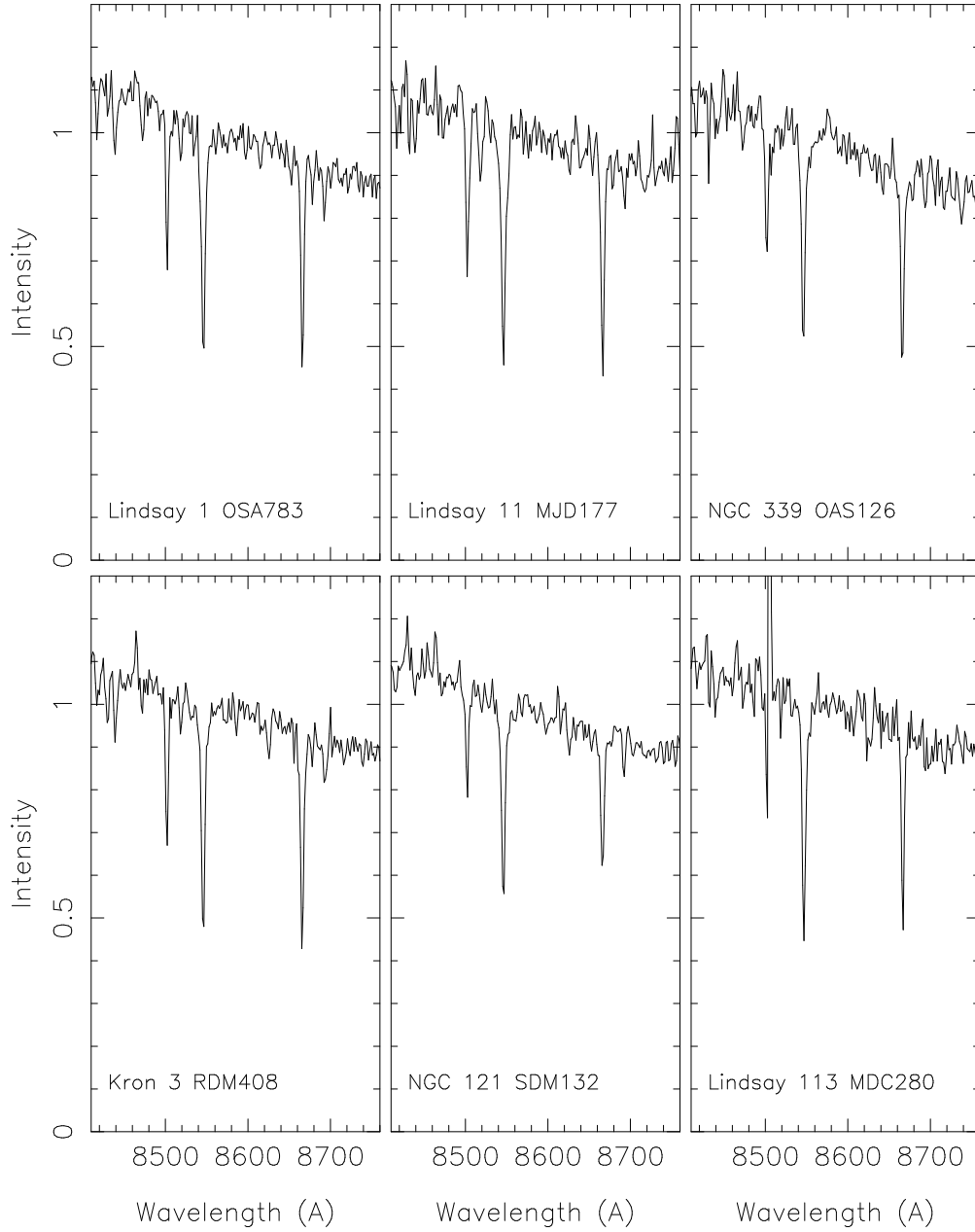


Fig. 1.— Examples of observed spectra for red giants in six SMC star clusters. The most prominent spectral features are the lines of the Ca II triplet at $\lambda 8498\text{\AA}$, $\lambda 8542\text{\AA}$ and $\lambda 8662\text{\AA}$. Each spectrum has been normalized to unity at $\sim 8600\text{\AA}$. The stars are identified in the panels. Note that the apparent emission feature near $\lambda 8498\text{\AA}$ in the spectrum of Lindsay 113 MDC280 is a cosmic ray artifact.

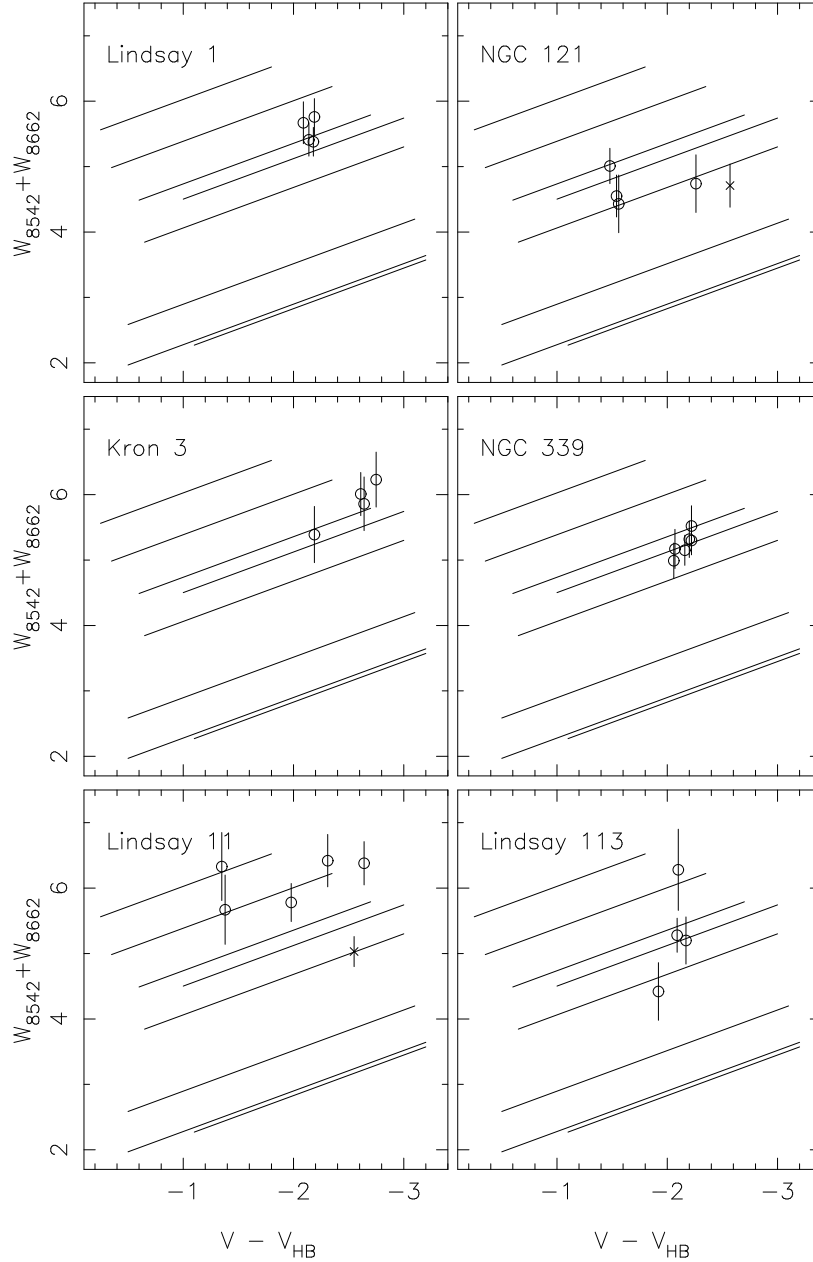


Fig. 2.— Plots of the Ca II line strength index $W_{8542} + W_{8662}$ in \AA against magnitude difference from the horizontal branch $V - V_{HB}$ for individual stars in the fields of six SMC star clusters. Probable cluster members are plotted as open circles while probable non-members are shown as \times -symbols. The lines in the panels are taken from Da Costa & Armandroff (1995) and represent the Ca II line strength, magnitude relations for galactic globular clusters. In order of increasing Ca II line strength, the clusters are M15, NGC 4590 (M68), NGC 6397, NGC 6752, M5, M4, 47 Tuc and NGC 5927. These clusters have abundances $[\text{Fe}/\text{H}]$ on the Zinn & West (1984) scale of -2.17 , -2.09 , -1.91 , -1.54 , -1.40 , -1.28 , -0.71 and -0.31 dex, respectively.

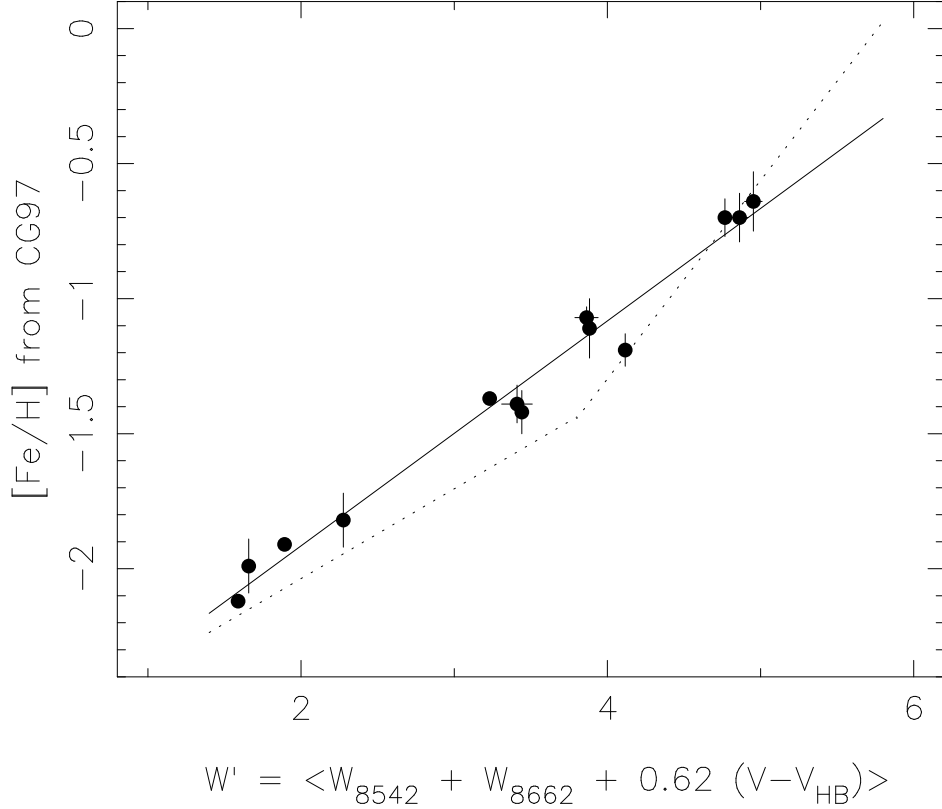


Fig. 3.— The reduced equivalent width W' in \AA is plotted against iron abundance $[\text{Fe}/\text{H}]$ from Carretta & Gratton (1997), if available, for the abundance calibration clusters of Da Costa & Armandroff (1995). These $[\text{Fe}/\text{H}]$ values all have their basis in high dispersion spectroscopy. The solid line is a least squares fit to the data. The dotted line is the two linear segment fit of DA95 to $[\text{Fe}/\text{H}]$ values on the scale of Zinn & West (1984). Note that for $W' \approx 3.8\text{\AA}$, the relations give $[\text{Fe}/\text{H}]$ values that differ by almost 0.3 dex.

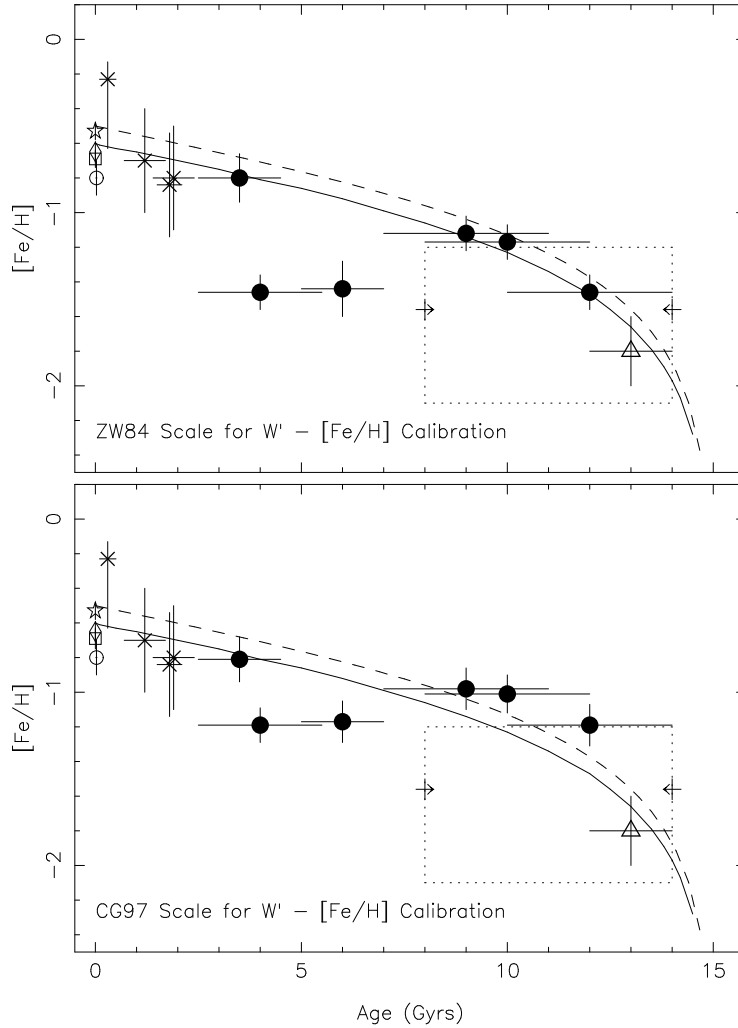


Fig. 4.— The age-metallicity relation for the SMC. Filled symbols are the clusters observed in this paper with abundances on the Zinn & West (1984) scale shown in the upper panel and on the Carretta & Gratton (1997) scale in the lower panel. The \times -symbols are the clusters, in order of increasing age, NGC 458, NGC 419, NGC 411 and NGC 152, respectively, while the open triangle is the SMC field RR Lyrae mean abundance of Butler *et al.* (1982). The arrow symbols indicate the mean abundance of SMC field red giants from Suntzeff *et al.* (1986) and the box outlined by the dotted lines indicates the range in abundance and age for these stars. The distribution of these stars within the box, however, is unknown. The star-, diamond- and square-symbols are spectroscopic results for the present-day abundance of the SMC from Luck & Lambert (1992), Russell & Bessell (1989) and Hill (1997), respectively, while the open circle is the cluster NGC 330 plotted using the abundance of Hill & Spite (1997). In both panels the solid and dashed lines are the relations predicted by simple chemical evolution models. Both curves use the same present-day gas mass fraction (0.36) and formation epoch (15 Gyr) but the model depicted by the solid line employs a present-day abundance of -0.6 dex, while that for the dashed line uses -0.5 dex.